Supplementary material for "Shift-current response as a probe of quantum geometry and electron-electron interactions in twisted bilayer graphene"

Swati Chaudhary[‡][*]

Department of Physics, California Institute of Technology, Pasadena CA 91125, USA
Institute for Quantum Information and Matter, California Institute of Technology, Pasadena CA 91125, USA
Department of Physics, The University of Texas at Austin, Austin, Texas 78712, USA
Department of Physics, Northeastern University, Boston, Massachusetts 02115, USA and
Department of Physics, Massachusetts Institute of Technology, Cambridge, Massachusetts 02139, USA

Cyprian Lewandowski[‡][†] and Gil Refael

Department of Physics, California Institute of Technology, Pasadena CA 91125, USA and
Institute for Quantum Information and Matter, California Institute of Technology, Pasadena CA 91125, USA

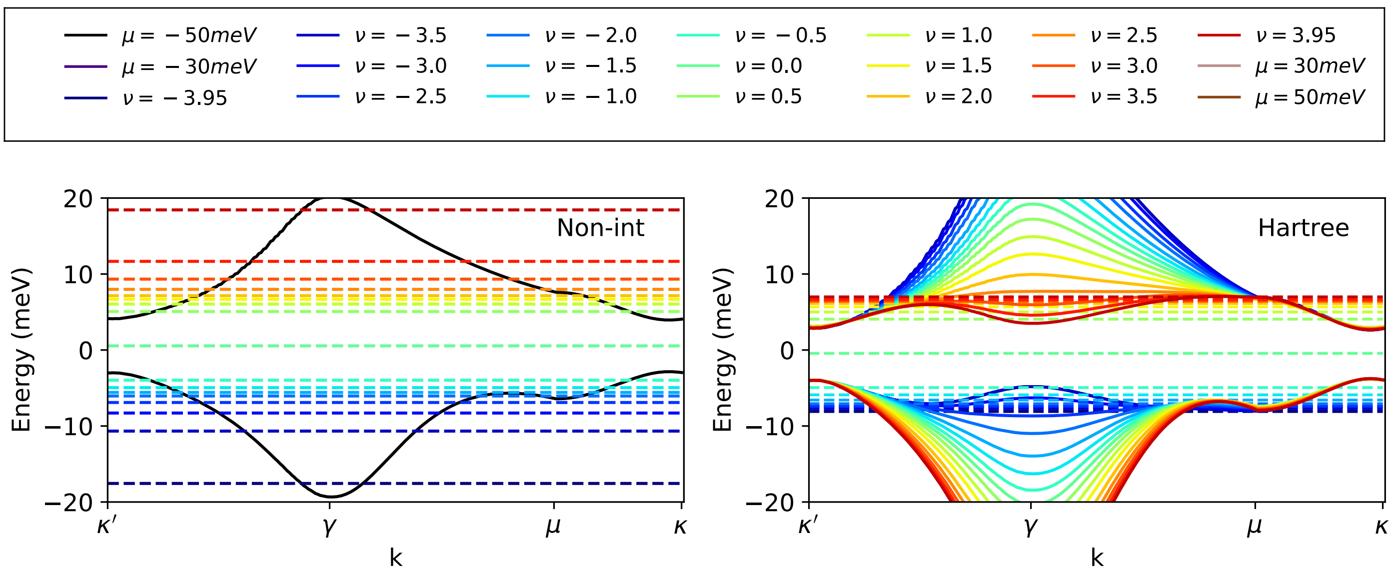

Supplemental Figure S1. **Chemical potential at different fillings:** The chemical potential at different fillings is shown on top of the band structure of twisted bilayer graphene with twist angle $\theta = 0.8^\circ$ for non-interacting (left) and interacting case (right).

Appendix A: Procedure for fitting TBG continuum model to scanning tunneling microscopy (STM) experiments

In this Appendix, we explain the fitting procedure used in Sec.III of the main text. The procedure follows closely the one adopted in Ref.[1] which is meant as an accompanying reference to this Appendix. The purpose of this modelling approach is to provide an experimentally inspired model which captures the qualitative behavior of electronic energies as a function of twist angle and filling, rather then to provide a complete and full treatment of interactions in TBG. Moreover, we focus here only on a Hartree correction, as motivated in the main text, since they dominate over a wider twist angle range as well as we expect them to be the leading interaction correction at the typical temperature associated with NLOR experiments (i.e. exchange effects are suppressed). We note however the large body of existing

* swati.chaudhary@austin.utexas.edu
† cyprian@caltech.edu

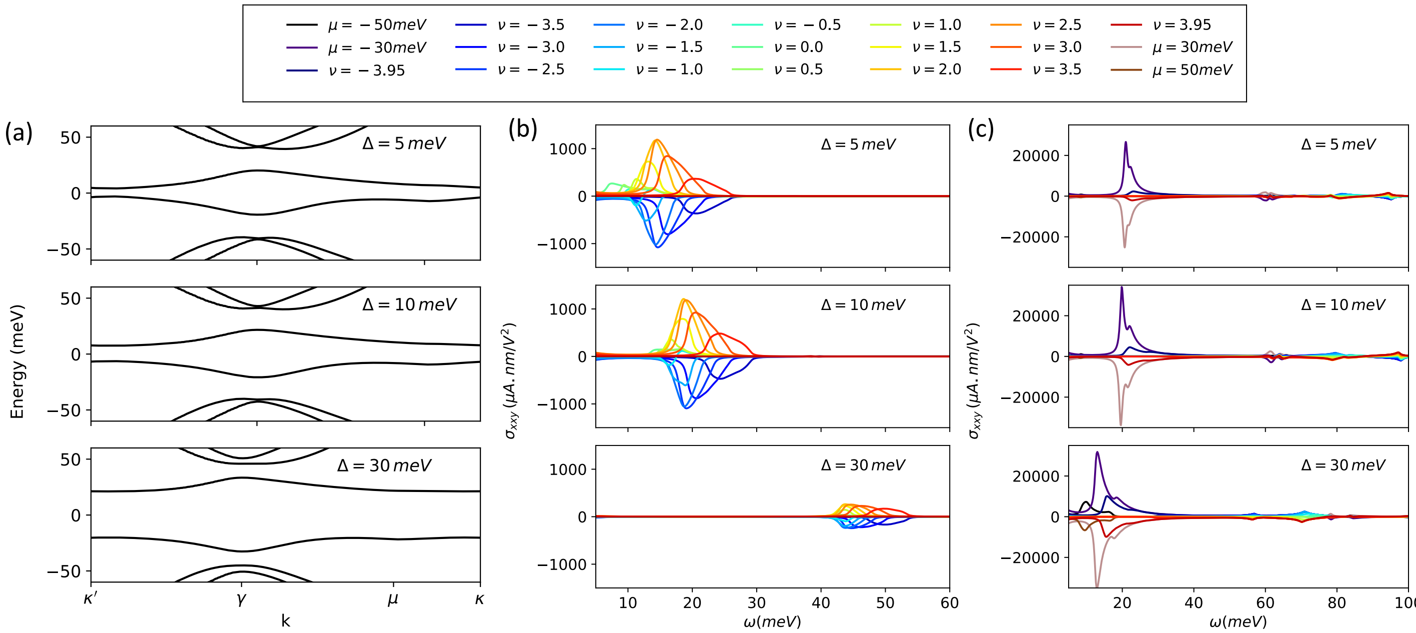

Supplemental Figure S2. **Effect of increasing sublattice offset energy Δ on energy spectrum and shift-current response :** (a) Energy spectrum around flat bands, (b) FF contribution to second-order conductivity, and (c) FD contribution to second-order conductivity of twisted bilayer graphene with twist angle, $\theta = 0.8°$, for three different sublattice offset energies. As Δ increases, the gap between flat bands increases but they come closer to the dispersive bands and it results in an opposite frequency shift for the peak value in FF and FD case.

work in the literature that analyzes Hartree-Fock contributions (e.g., Refs. [2–7]). Lastly, we also point out that the modelling of Ref.[1] focuses solely on TBG without substrate induced gap Δ, which here we treat as a free parameter. Given that the inhomogeneous charge distribution present in the moiré unit cell is weakly affected by Δ, we expect the behaviour of Hartree interaction to remain similar to the one studied in Ref.[1].

The non-interacting continuum model introduced in the Sec.III has two free parameters, the interlayer couplings u, u', for a given twist angle θ. While the dependence on twist angle of these parameters has been studied through ab-initio methods [8], in our modelling we choose a simpler approach intended to highlight the interaction-driven qualitative changes to the band structure. Specifically, we assume the same-sublattice (u) and opposite-sublattice (u') interlayer tunneling parameters have fixed values for all twist angles. We caution that this approximation misses the subtle role relaxation physics plays on increasing the ratio of these parameters $\eta = u/u'$ as the twist angle is brought closer to the magic angle [8]. Crucially, however the resulting charge density profiles that give rise to the Hartree corrections are weakly affected by changes in these parameters making our conclusions robust. Moreover, we expect that the twist dependent ratio of $\eta = u/u'$ will not qualitatively alter our results when studied as a function of filling ν. Specifically, the location of van Hove singularities in each band does not change with η for values of $\eta \lesssim 0.8$ (See also discussion in Ref. [9]). To fix u and u', we focus on the measurements at the largest available angle of $\theta = 1.32°$ in Ref.[1], where the role of interactions is least important. By matching the measured Landau-level (LL) spectrum to that obtained numerically from this continuum model, we fix $u' = 90$ meV and $u = 0.4u'$. As noted in the main text, as a result of this approximation scheme the magic-angle of the non-interacting model occurs at $\theta \approx 0.99°$ differing from the typical values $\theta \approx 1.1°$ quoted in the literature.

We now explain the procedure used to determine value of the dielectric screening ε in the Coulomb potential $\mathcal{V}_c(q) = 2\pi e^2/\varepsilon q$. Microscopically its value is set by the substrate— for a typical hBN encapsulated graphene its value would be $\varepsilon \approx 5$. This ε however massively overestimates the role of Hartree and Fock processes, leading to band structures with large γ point inversions that are not observed experimentally. To overcome this unwarranted behavior, earlier works [2, 7, 10] use a wider range of values for ε. Following this procedure, we choose $\varepsilon = 15$ to quantitatively capture the following three experimental characteristics seen in the LL spectra of Ref.[1]: (i) the energy spacing between LLs arising from the γ point band structure at $\theta = 1.32°$ (Fig. 1 in Ref.[1]), (ii) the energy spacing between the highest energy LL from the flat band and the lowest energy LL from the dispersive bands at $\theta = 1.32°$ (Fig. 1 in Ref.[1]), and (iii) the critical angle at which largest energy LL from the flat-band joins the vHs (Fig. 2 in Ref.[1]). These criteria are met with a choice of $\varepsilon = 15$, which is then kept constant for all values of θ. As argued in Ref.[1] such parameterized Coulomb interaction, i.e. one that includes Hartree-only correction, adequately captures experimental observations for twist angles away from the magic angle, suggesting that the Fock term plays a subdominant role for such θ. In the vicinity of the magic angle, one expects the exchange effects to become significant and, amongst a wide number of correlated effects, to also introduce band broadening and counteract the Hartree driven band inversion at the γ point (See discussion in Ref. [1]).

For the bandstructures and calculations presented in this paper, we evaluate the solutions for all fillings self-consistently until convergence is reached. We set the convergence threshold for all self-consistent parameters as 0.1% total relative error (difference between successive self-consistent steps). A grid of 441 k-points was used for the analysis of the self-consistent potentials, where the convergence reached after a few (typically in less than 5) iterations.

Appendix B: Shift-current expressions

In this section, we derive expressions for shift-current expressions using velocity gauge. There are mainly two different approaches to calculate the shift-current response. The first approach is based on evaluating the shift-vector directly from the Berry connection. However, a direct numerical evaluation of Berry connection can be severely affected by the gauge fixing issues. On the other hand, one can also evaluate this response directly from the matrix elements of different k space derivatives of the Hamiltonian. The expressions obtained from this second approach are insensitive to the gauge used. We noticed that different references use different forms of these expressions which can lead to confusion. Here, we elucidate the connection between different expressions and also highlight the importance of physical processes associated with different terms appearing in this derivation.

Within the independent particle approximation and using minimal coupling approach, the second-order conductivity for a perturbation arising from a linearly polarized EM field can be obtained using formula Eq. 43 of Ref.[11]

$$\begin{aligned}\sigma^{\mu}_{\alpha\beta}(\omega_Z,\omega_1,\omega_2) = &-\frac{e^3}{\hbar^2\omega_1\omega_2}\sum_{a,b,c}\int d\mathbf{k}\, \frac{1}{2}f_a h^{\mu\alpha\beta}_{aa} + \frac{1}{2}f_a h^{\mu\beta\alpha}_{aa} + f_{ab}\frac{h^{\alpha}_{ab}h^{\mu\beta}_{ba}}{\omega_1-\varepsilon_{ab}} + f_{ab}\frac{h^{\beta}_{ab}h^{\mu\alpha}_{ba}}{\omega_2-\varepsilon_{ab}} + \frac{1}{2}f_{ab}\frac{h^{\alpha\beta}_{ab}h^{\mu}_{ba}}{\omega_Z-\varepsilon_{ab}} \\ &+\frac{1}{2}f_{ab}\frac{h^{\beta\alpha}_{ab}h^{\mu}_{ba}}{\omega_Z-\varepsilon_{ab}} + \frac{h^{\alpha}_{ab}h^{\beta}_{bc}h^{\mu}_{ca}}{\omega_Z-\varepsilon_{ca}}\left[\frac{f_{ab}}{\omega_1-\varepsilon_{ba}}+\frac{f_{cb}}{\omega_2-\varepsilon_{cb}}\right] + \frac{h^{\beta}_{ab}h^{\alpha}_{bc}h^{\mu}_{ca}}{\omega_Z-\varepsilon_{ca}}\left[\frac{f_{ab}}{\omega_2-\varepsilon_{ba}}+\frac{f_{cb}}{\omega_1-\varepsilon_{cb}}\right]\end{aligned} \tag{B1}$$

where $\omega_Z=\omega_1+\omega_2$, $h^{\alpha}_{ab}=\langle a|\nabla_{k_\alpha}H|b\rangle$, $h^{\alpha\beta}_{ab}=\langle a|\nabla_{k_\alpha}\nabla_{k_\beta}H|b\rangle$ are derivatives of hamiltonian, $\varepsilon_{ab}=\varepsilon_a-\varepsilon_b$ is the energy difference, and $f_{ab}=f_a-f_b$ is the difference in occupancy of energy level a and b. This formula many different contributions like injection current, shift current etc. It can be recast in a slightly different form by shifting all frequencies by $\omega\to\omega+i\eta$ and the above equation reduces to

$$\begin{aligned}\sigma^{\mu}_{\alpha\beta}(\omega_Z,\omega_1,\omega_2) = &-\frac{e^3}{\hbar^2\omega_1\omega_2}\sum_{a,b,c}\int d\mathbf{k}\, \frac{1}{2}f_a h^{\mu\alpha\beta}_{aa} + \frac{1}{2}f_a h^{\mu\beta\alpha}_{aa} + f_{ab}\frac{h^{\alpha}_{ab}h^{\mu\beta}_{ba}}{\omega_1+i\eta-\varepsilon_{ab}} + f_{ab}\frac{h^{\beta}_{ab}h^{\mu\alpha}_{ba}}{\omega_2+i\eta-\varepsilon_{ab}} + \frac{1}{2}f_{ab}\frac{h^{\alpha\beta}_{ab}h^{\mu}_{ba}}{\omega_Z+i\eta-\varepsilon_{ab}} \\ &+\frac{1}{2}f_{ab}\frac{h^{\beta\alpha}_{ab}h^{\mu}_{ba}}{\omega_Z+i\eta-\varepsilon_{ab}} + \frac{h^{\alpha}_{ab}h^{\beta}_{bc}h^{\mu}_{ca}}{\omega_Z+i\eta-\varepsilon_{ca}}\left[\frac{f_{ab}}{\omega_1+i\eta-\varepsilon_{ba}}+\frac{f_{cb}}{\omega_2+i\eta-\varepsilon_{cb}}\right] + \frac{h^{\beta}_{ab}h^{\alpha}_{bc}h^{\mu}_{ca}}{\omega_Z+i\eta-\varepsilon_{ca}}\left[\frac{f_{ab}}{\omega_2+i\eta-\varepsilon_{ba}}+\frac{f_{cb}}{\omega_1+i\eta-\varepsilon_{cb}}\right]\end{aligned} \tag{B2}$$

The DC response to an AC field of frequency ω is given by $\sigma^{\mu}_{\alpha\beta}(0,\omega,-\omega)$. which can be obtained from Eq. B2 by substituting $\omega_1=-\omega_2=\omega$ and for our prime case of interest ($\alpha=\beta$), we get

$$\begin{aligned}\sigma^{\mu}_{\alpha\alpha}(0,\omega,-\omega) = &\frac{e^3}{\hbar^2\omega^2}\sum_{a,b,c}\int d\mathbf{k}\, f_a h^{\mu\alpha\alpha}_{aa} + f_{ab}\frac{h^{\alpha}_{ab}h^{\mu\alpha}_{ba}}{\omega+i\eta-\varepsilon_{ab}} + f_{ab}\frac{h^{\alpha}_{ab}h^{\mu\alpha}_{ba}}{-\omega+i\eta-\varepsilon_{ab}} + f_{ab}\frac{h^{\alpha\alpha}_{ab}h^{\mu}_{ba}}{\varepsilon_{ba}} \\ &+\frac{h^{\alpha}_{ab}h^{\alpha}_{bc}h^{\mu}_{ca}}{\varepsilon_{ac}}\left[\frac{f_{ab}}{\omega+i\eta-\varepsilon_{ba}}+\frac{f_{cb}}{-\omega+i\eta-\varepsilon_{cb}}\right] + \frac{h^{\alpha}_{ab}h^{\alpha}_{bc}h^{\mu}_{ca}}{\varepsilon_{ac}}\left[\frac{f_{ab}}{-\omega+i\eta-\varepsilon_{ba}}+\frac{f_{cb}}{\omega+i\eta-\varepsilon_{cb}}\right]\end{aligned} \tag{B3}$$

1. Connections with shift current expression

In order to understand the connections between the shift-current expression we encountered in the main text and the form the second-order conductivity considered above, we can first split this equation into two different kind of contributions

$$\sigma^{\mu}_{\alpha\alpha}(0,\omega,-\omega) = \frac{e^2}{\hbar^2\omega^2}\sum_{a,b,c}\int d\mathbf{k}\, f_a h^{\mu\alpha\alpha}_{aa} + \underbrace{f_{ab}\frac{h^{\alpha}_{ab}h^{\mu\alpha}_{ba}}{\omega+i\eta-\varepsilon_{ab}} + f_{ab}\frac{h^{\alpha}_{ab}h^{\mu\alpha}_{ba}}{-\omega+i\eta-\varepsilon_{ab}}}_{\sigma^{23}} + f_{ab}\frac{h^{\alpha\alpha}_{ab}h^{\mu}_{ba}}{\varepsilon_{ba}} + \underbrace{\frac{h^{\alpha}_{ab}h^{\alpha}_{bc}h^{\mu}_{ca}}{\varepsilon_{ac}}\left[\frac{f_{ab}}{\omega+i\eta-\varepsilon_{ba}} + \frac{f_{cb}}{-\omega+i\eta-\varepsilon_{cb}}\right] + \frac{h^{\alpha}_{ab}h^{\alpha}_{bc}h^{\mu}_{ca}}{\varepsilon_{ac}}\left[\frac{f_{ab}}{-\omega+i\eta-\varepsilon_{ba}} + \frac{f_{cb}}{\omega+i\eta-\varepsilon_{cb}}\right]}_{\sigma^{56}} \tag{B4}$$

Let's first focus on 2nd and 3rd term of Eq. B4, σ^{23}, where the integrand can be expressed as

$$\begin{aligned} f_{ab}\frac{h^{\alpha}_{ab}h^{\mu\alpha}_{ba}}{\omega+i\eta-\varepsilon_{ab}} + f_{ab}\frac{h^{\alpha}_{ab}h^{\mu\alpha}_{ba}}{-\omega+i\eta-\varepsilon_{ab}} = f_{ab}\frac{h^{\alpha}_{ab}h^{\mu\alpha}_{ba}}{\omega+i\eta-\varepsilon_{ab}} - f_{ba}\frac{h^{\alpha}_{ba}h^{\mu\alpha}_{ab}}{\omega-i\eta+\varepsilon_{ba}} = f_{ab}\frac{h^{\alpha}_{ab}h^{\mu\alpha}_{ba}}{\omega+i\eta-\varepsilon_{ab}} + \\ f_{ab}\frac{h^{\alpha}_{ba}h^{\mu\alpha}_{ab}}{\omega-i\eta-\varepsilon_{ab}} = f_{ab}P\left(\frac{1}{\omega-\varepsilon_{ab}}\right)\left[h^{\alpha}_{ab}h^{\mu\alpha}_{ba} + h^{\alpha}_{ba}h^{\mu\alpha}_{ab}\right] + f_{ab}i\pi\left[h^{\alpha}_{ab}h^{\mu\alpha}_{ba} - h^{\alpha}_{ba}h^{\mu\alpha}_{ab}\right]\delta(\omega-\varepsilon_{ab}) \end{aligned} \tag{B5}$$

For our purpose, the most interesting term is the one involving $\delta(\omega-\varepsilon_{ab})$. We can write

$$h^{\alpha}_{ab}h^{\mu\alpha}_{ba} - h^{\alpha}_{ba}h^{\mu\alpha}_{ab} = h^{\alpha}_{ab}h^{\mu\alpha}_{ba} - [a \leftrightarrow b]. \tag{B6}$$

Now, first we derive an expression for $h^{\alpha\beta}_{mn}$. According to the notation used in Ref. [11],

$$h^{\alpha\beta}_{mn} = \left[D^{\alpha}D^{\beta}[H_0]\right]_{mn} \equiv \langle m|\nabla_{\alpha}\nabla_{\beta}(H_0)|n\rangle \tag{B7}$$

where H_0 is the unperturbed hamiltonian and for a given operator O

$$D[O]_{ab} = [D,O]_{ab} = \nabla_k(O_{ab}) - i[\mathbf{A},O]_{ab} \tag{B8}$$

where $\mathbf{A}$ is the Berry-connection matrix with $\mathbf{A}^{\mu}_{mn} = i\langle u_m|\partial_{k^{\mu}}|u_n\rangle$. We can thus write

$$h^{\alpha\beta}_{mn} = \left[D^{\alpha}D^{\beta}[H_0]\right]_{mn} = \partial_{\alpha}\left(\left[D^{\beta}[H_0]\right]_{mn}\right) - i\left[\mathbf{A}^{\alpha}, D^{\beta}[H_0]\right]_{mn}. \tag{B9}$$

We have

$$h^{\beta}_{mn} = \left(D^{\beta}[H_0]\right)_{mn} = \partial_{\beta}((H_0)_{mn}) - i\left[\mathbf{A}^{\beta}, H_0\right]_{mn} = \underbrace{\delta_{mn}v^{\beta}_{nn} - i(\varepsilon_n-\varepsilon_m)\mathbf{A}^{\beta}_{mn}}_{v^{\beta}_{mn}} \tag{B10}$$

where we have used the fact that $\langle m|H_0|n\rangle = \delta_{mn}\varepsilon_n$ and $v^{\beta}_{nn} = \partial_{\beta}\varepsilon_n$. We can express

$$\left[\mathbf{A}^{\alpha}, D^{\beta}[H_0]\right]_{mn} = \left[\mathbf{A}^{\alpha}h^{\beta} - h^{\beta}\mathbf{A}^{\alpha}\right]_{mn} = \mathbf{A}^{\alpha}_{md}h^{\beta}_{dn} - \mathbf{A}^{\alpha}_{dn}h^{\beta}_{md} \tag{B11}$$

For the first term in Eq. B9, we can use Eq. B10 to write

$$\partial_{\alpha}\left(\left[D^{\beta}[H_0]\right]_{mn}\right) = \delta_{mn}\partial_{\alpha}\varepsilon_n - i(v^{\alpha}_{nn}-v^{\alpha}_{mm})\mathbf{A}^{\beta}_{mn} - i\varepsilon_{nm}\partial_{\alpha}\mathbf{A}^{\beta}_{mn} \tag{B12}$$

and the second part can be fully extended using Eq. B10 and Eq. B11

$$-i\left[\mathbf{A}^{\alpha}, D^{\beta}[H_0]\right]_{mn} = -i\mathbf{A}^{\alpha}_{md}\left(\delta_{dn}v^{\beta}_{nn} - i\varepsilon_{nd}\mathbf{A}^{\beta}_{db}\right) + i\mathbf{A}^{\alpha}_{dn}\left(\delta_{md}v^{\beta}_{mm} - i\varepsilon_{dm}\mathbf{A}^{\beta}_{md}\right) \tag{B13}$$

Now, combining these two equations we get:

$$\begin{aligned} h^{\alpha\beta}_{mn} = \partial_{\alpha}\left(\left[D^{\beta}[H_0]\right]_{mn}\right) - i\left[\mathbf{A}^{\alpha}, D^{\beta}[H_0]\right]_{mn} = \delta_{mn}\partial_{\alpha}\varepsilon_n - i(v^{\alpha}_{nn}-v^{\alpha}_{mm})\mathbf{A}^{\beta}_{mn} - i\varepsilon_{nm}\partial_{\alpha}\mathbf{A}^{\beta}_{mn} \\ -i\mathbf{A}^{\alpha}_{md}\delta_{dn}v^{\beta}_{nn} + i\mathbf{A}^{\alpha}_{dn}\delta_{md}v^{\beta}_{mm} - \varepsilon_{nd}\mathbf{A}^{\alpha}_{md}\mathbf{A}^{\beta}_{dn} + \varepsilon_{dm}\mathbf{A}^{\alpha}_{dn}\mathbf{A}^{\beta}_{md}. \end{aligned} \tag{B14}$$

$$\begin{aligned} h^{\alpha\beta}_{mn} = \partial_{\alpha}\left(\left[D^{\beta}[H_0]\right]_{mn}\right) - i\left[\mathbf{A}^{\alpha}, D^{\beta}[H_0]\right]_{mn} = \delta_{mn}\partial_{\alpha}\varepsilon_n - i(v^{\alpha}_{nn}-v^{\alpha}_{mm})\mathbf{A}^{\beta}_{mn} - i\varepsilon_{nm}\partial_{\alpha}\mathbf{A}^{\beta}_{mn} \\ -i\mathbf{A}^{\alpha}_{mn}v^{\beta}_{nn} + i\mathbf{A}^{\alpha}_{mn}v^{\beta}_{mm} - \varepsilon_{nd}\mathbf{A}^{\alpha}_{md}\mathbf{A}^{\beta}_{dn} + \varepsilon_{dm}\mathbf{A}^{\alpha}_{dn}\mathbf{A}^{\beta}_{md}. \end{aligned} \tag{B15}$$

Our goal was to evaluate $h^{\alpha}_{ab}h^{\mu\alpha}_{ba}$ in Eq. B6. For now, we are going to focus on case $a \neq b$ For $a \neq b$, $h^{\alpha}_{ab} = -i\varepsilon_{ba}\mathbf{A}^{\alpha}_{ab}$ from Eq. B10 and similarly

$$h^{\alpha}_{ab}h^{\mu\alpha}_{ba} = -i\varepsilon_{ba}\mathbf{A}^{\alpha}_{ab}\left(-i\Delta^{\mu}_{ab}\mathbf{A}^{\alpha}_{ba} - i\varepsilon_{ab}\partial_{\mu}\mathbf{A}^{\alpha}_{ba} - i\mathbf{A}^{\mu}_{ba}\Delta^{\alpha}_{ab} - \varepsilon_{ad}\mathbf{A}^{\mu}_{bd}\mathbf{A}^{\alpha}_{da} + \varepsilon_{db}\mathbf{A}^{\mu}_{da}\mathbf{A}^{\alpha}_{bd}\right). \tag{B16}$$

where $\Delta^{\mu}_{ab} = v^{\mu}_{aa} - v^{\mu}_{bb}$. This gives

$$\begin{aligned} h^{\alpha}_{ab}h^{\mu\alpha}_{ba} - h^{\alpha}_{ba}h^{\mu\alpha}_{ab} = \varepsilon^2_{ab}\left(\mathbf{A}^{\alpha}_{ab}\partial_{\mu}\mathbf{A}^{\alpha}_{ba} - \mathbf{A}^{\alpha}_{ba}\partial_{\mu}\mathbf{A}^{\alpha}_{ab}\right) - \varepsilon_{ba}\Delta^{\alpha}_{ab}\left(\mathbf{A}^{\alpha}_{ab}\mathbf{A}^{\mu}_{ba} - \mathbf{A}^{\alpha}_{ba}\mathbf{A}^{\mu}_{ab}\right) \\ -i\varepsilon_{ba}\left(-\varepsilon_{ad}\mathbf{A}^{\alpha}_{ab}\mathbf{A}^{\mu}_{bd}\mathbf{A}^{\alpha}_{da} - \varepsilon_{bd}\mathbf{A}^{\alpha}_{ba}\mathbf{A}^{\mu}_{ad}\mathbf{A}^{\alpha}_{db}\right) - i\varepsilon_{ba}\left(\varepsilon_{db}\mathbf{A}^{\alpha}_{ab}\mathbf{A}^{\mu}_{da}\mathbf{A}^{\alpha}_{bd} + \varepsilon_{da}\mathbf{A}^{\alpha}_{ba}\mathbf{A}^{\mu}_{db}\mathbf{A}^{\alpha}_{ad}\right) \end{aligned} \tag{B17}$$

It can be written as

$$\begin{aligned} h^{\alpha}_{ab}h^{\mu\alpha}_{ba} - h^{\alpha}_{ba}h^{\mu\alpha}_{ab} = 2i\varepsilon^2_{ab}\left(|\mathbf{A}^{\alpha}_{ab}|^2\partial_{\mu}\varphi^{\alpha}_{ba}\right) - \varepsilon_{ba}\Delta^{\alpha}_{ab}\left(\mathbf{A}^{\alpha}_{ab}\mathbf{A}^{\mu}_{ba} - \mathbf{A}^{\alpha}_{ba}\mathbf{A}^{\mu}_{ab}\right) \\ -i\varepsilon_{ba}\left(-\varepsilon_{ab}\mathbf{A}^{\alpha}_{ab}\mathbf{A}^{\mu}_{bb}\mathbf{A}^{\alpha}_{ba} - \varepsilon_{ba}\mathbf{A}^{\alpha}_{ba}\mathbf{A}^{\mu}_{aa}\mathbf{A}^{\alpha}_{ab}\right) - i\varepsilon_{ba}\left(\varepsilon_{ab}\mathbf{A}^{\alpha}_{ab}\mathbf{A}^{\mu}_{aa}\mathbf{A}^{\alpha}_{ba} + \varepsilon_{ba}\mathbf{A}^{\alpha}_{ba}\mathbf{A}^{\mu}_{bb}\mathbf{A}^{\alpha}_{ab}\right) \\ \sum_{d\neq a,b} -i\varepsilon_{ba}\left(-\varepsilon_{ad}\mathbf{A}^{\alpha}_{ab}\mathbf{A}^{\mu}_{bd}\mathbf{A}^{\alpha}_{da} - \varepsilon_{bd}\mathbf{A}^{\alpha}_{ba}\mathbf{A}^{\mu}_{ad}\mathbf{A}^{\alpha}_{db}\right) - i\varepsilon_{ba}\left(\varepsilon_{db}\mathbf{A}^{\alpha}_{ab}\mathbf{A}^{\mu}_{da}\mathbf{A}^{\alpha}_{bd} + \varepsilon_{da}\mathbf{A}^{\alpha}_{ba}\mathbf{A}^{\mu}_{db}\mathbf{A}^{\alpha}_{ad}\right) \end{aligned} \tag{B18}$$

where $\varphi^{\mu}_{ba} = \mathrm{Arg}[\mathbf{A}^{\mu}_{ba}]$, and simplifying it further we get

$$\begin{aligned} h^{\alpha}_{ab}h^{\mu\alpha}_{ba} - h^{\alpha}_{ba}h^{\mu\alpha}_{ab} = 2i\varepsilon^2_{ab}\left(|\mathbf{A}^{\alpha}_{ab}|^2\partial_{\mu}\varphi^{\alpha}_{ba}\right) - 2i\varepsilon^2_{ba}\left|\mathbf{A}^{\alpha}_{ab}\right|^2\left(\mathbf{A}^{\mu}_{bb} - \mathbf{A}^{\mu}_{aa}\right) - \varepsilon_{ba}\Delta^{\alpha}_{ab}\left(\mathbf{A}^{\alpha}_{ab}\mathbf{A}^{\mu}_{ba} - \mathbf{A}^{\alpha}_{ba}\mathbf{A}^{\mu}_{ab}\right) \\ \sum_{d\neq a,b} -i\varepsilon_{ba}\left(-\varepsilon_{ad}\mathbf{A}^{\alpha}_{ab}\mathbf{A}^{\mu}_{bd}\mathbf{A}^{\alpha}_{da} - \varepsilon_{bd}\mathbf{A}^{\alpha}_{ba}\mathbf{A}^{\mu}_{ad}\mathbf{A}^{\alpha}_{db}\right) - i\varepsilon_{ba}\left(\varepsilon_{db}\mathbf{A}^{\alpha}_{ab}\mathbf{A}^{\mu}_{da}\mathbf{A}^{\alpha}_{bd} + \varepsilon_{da}\mathbf{A}^{\alpha}_{ba}\mathbf{A}^{\mu}_{db}\mathbf{A}^{\alpha}_{ad}\right) \end{aligned} \tag{B19}$$

Now, we can further simplify it by using $h^{\gamma}_{mn} = i\varepsilon_{nm}\mathbf{A}^{\gamma}_{mn}$ for $m \neq n$,

$$\begin{aligned} h^{\alpha}_{ab}h^{\mu\alpha}_{ba} - h^{\alpha}_{ba}h^{\mu\alpha}_{ab} = -2i\varepsilon^2_{ab}|\mathbf{A}^{\alpha}_{ab}|^2\underbrace{\left(\mathbf{A}^{\mu}_{bb} - \mathbf{A}^{\mu}_{aa} - \partial_{\mu}\varphi^{\alpha}_{ba}\right)}_{\text{Shift vector, } \mathbf{S}^{\mu}_{ba}} - \varepsilon_{ba}\Delta^{\alpha}_{ab}\left(\mathbf{A}^{\alpha}_{ab}\mathbf{A}^{\mu}_{ba} - \mathbf{A}^{\alpha}_{ba}\mathbf{A}^{\mu}_{ab}\right) \\ \sum_{d\neq a,b}\left(-\varepsilon_{ad}h^{\alpha}_{ab}\mathbf{A}^{\mu}_{bd}\mathbf{A}^{\alpha}_{da} + \varepsilon_{bd}h^{\alpha}_{ba}\mathbf{A}^{\mu}_{ad}\mathbf{A}^{\alpha}_{db}\right) + \left(\varepsilon_{db}h^{\alpha}_{ab}\mathbf{A}^{\mu}_{da}\mathbf{A}^{\alpha}_{bd} - \varepsilon_{da}h^{\alpha}_{ba}\mathbf{A}^{\mu}_{db}\mathbf{A}^{\alpha}_{ad}\right). \end{aligned} \tag{B20}$$

It can be simplified further

$$\begin{aligned} h^{\alpha}_{ab}h^{\mu\alpha}_{ba} - h^{\alpha}_{ba}h^{\mu\alpha}_{ab} = -2i\varepsilon^2_{ab}|\mathbf{A}^{\alpha}_{ab}|^2\mathbf{S}^{\mu}_{ba} + \Delta^{\alpha}_{ab}\left(\frac{1}{\varepsilon_{ab}}h^{\alpha}_{ab}h^{\mu}_{ba} + \frac{1}{\varepsilon_{ba}}h^{\alpha}_{ba}h^{\mu}_{ab}\right) \\ \sum_{d\neq a,b}\left(-\frac{1}{\varepsilon_{bd}}h^{\alpha}_{ab}h^{\mu}_{bd}h^{\alpha}_{da} + \frac{1}{\varepsilon_{ad}}h^{\alpha}_{ba}h^{\mu}_{ad}h^{\alpha}_{db}\right) + \left(\frac{1}{\varepsilon_{da}}h^{\alpha}_{ab}h^{\mu}_{da}h^{\alpha}_{bd} - \frac{1}{\varepsilon_{db}}h^{\alpha}_{ba}h^{\mu}_{db}h^{\alpha}_{ad}\right). \end{aligned} \tag{B21}$$

Now substituting it back in $\delta(\omega - \varepsilon_{ab})$ part of Eq. B5, we get the contribution of 2nd and 3rd term of Eq. B4

$$\begin{aligned} \sigma^{23}_{\delta(\omega-\varepsilon_{ab})} = \frac{2\pi e^3}{\hbar^2}\int[d\mathbf{k}]f_{ab}|\mathbf{A}^{\alpha}_{ab}|^2\mathbf{S}^{\mu}_{ba}\delta(\omega - \varepsilon_{ab}) + \boxed{\frac{2\pi e^3}{\hbar^2\omega^2}\int[d\mathbf{k}]f_{ab}\Delta^{\alpha}_{ab}\left(\frac{1}{\varepsilon_{ab}}h^{\alpha}_{ab}h^{\mu}_{ba} + \frac{1}{\varepsilon_{ba}}h^{\alpha}_{ba}h^{\mu}_{ab}\right)i\delta(\omega - \varepsilon_{ab})} \\ \boxed{+\frac{2\pi e^3}{\hbar^2\omega^2}\sum_{d\neq a,b}\int[d\mathbf{k}]f_{ab}\left[\left(-\frac{1}{\varepsilon_{bd}}h^{\alpha}_{ab}h^{\mu}_{bd}h^{\alpha}_{da} + \frac{1}{\varepsilon_{ad}}h^{\alpha}_{ba}h^{\mu}_{ad}h^{\alpha}_{db}\right) + \left(\frac{1}{\varepsilon_{da}}h^{\alpha}_{ab}h^{\mu}_{da}h^{\alpha}_{bd} - \frac{1}{\varepsilon_{db}}h^{\alpha}_{ba}h^{\mu}_{db}h^{\alpha}_{ad}\right)\right]i\delta(\omega - \varepsilon_{ab})} \end{aligned} \tag{B22}$$

It is worth mentioning that the quantity $\Delta^{\alpha}_{ab}\left(\frac{1}{\varepsilon_{ab}}h^{\alpha}_{ab}h^{\mu}_{ba} + \frac{1}{\varepsilon_{ba}}h^{\alpha}_{ba}h^{\mu}_{ab}\right)$ and $\left[\left(-\frac{1}{\varepsilon_{bd}}h^{\alpha}_{ab}h^{\mu}_{bd}h^{\alpha}_{da} + \frac{1}{\varepsilon_{ad}}h^{\alpha}_{ba}h^{\mu}_{ad}h^{\alpha}_{db}\right) + \left(\frac{1}{\varepsilon_{da}}h^{\alpha}_{ab}h^{\mu}_{da}h^{\alpha}_{bd} - \frac{1}{\varepsilon_{db}}h^{\alpha}_{ba}h^{\mu}_{db}h^{\alpha}_{ad}\right)\right]$ are imaginary by default. This shows that the second and third term of Eq. B4 contains not only the shift vector term but also a few extra terms which include three velocity elements. Next, we would like to check if these extra terms shown in the box above cancel out σ^{56} (5th and 6th terms) of Eq. B4. We have

$$\sigma^{56} = \frac{2\pi e^3}{\hbar^2\omega^2}\int[d\mathbf{k}]\frac{h^{\alpha}_{ab}h^{\alpha}_{bc}h^{\mu}_{ca}}{\varepsilon_{ac}}\left[\frac{f_{ab}}{\omega + i\eta - \varepsilon_{ba}} + \frac{f_{cb}}{-\omega + i\eta - \varepsilon_{cb}}\right] + \frac{h^{\alpha}_{ab}h^{\alpha}_{bc}h^{\mu}_{ca}}{\varepsilon_{ac}}\left[\frac{f_{ab}}{-\omega + i\eta - \varepsilon_{ba}} + \frac{f_{cb}}{\omega + i\eta - \varepsilon_{cb}}\right] \tag{B23}$$

and after switching $a \leftrightarrow c$ in 3rd and 4th term,it can be written as

$$\sigma^{56} = \frac{2\pi e^3}{\hbar^2\omega^2}\int [d\mathbf{k}] \frac{f_{ab}}{\varepsilon_{ac}} \frac{h^\alpha_{ab}h^\alpha_{bc}h^\mu_{ca}}{\omega + i\eta - \varepsilon_{ba}} + \frac{f_{ab}}{\varepsilon_{ca}} \frac{h^\alpha_{cb}h^\alpha_{ba}h^\mu_{ac}}{-\omega + i\eta - \varepsilon_{ab}} + \frac{f_{ab}}{\varepsilon_{ac}} \frac{h^\alpha_{ab}h^\alpha_{bc}h^\mu_{ca}}{-\omega + i\eta - \varepsilon_{ba}} + \frac{f_{ab}}{\varepsilon_{ca}} \frac{h^\alpha_{cb}h^\alpha_{ba}h^\mu_{ac}}{\omega + i\eta - \varepsilon_{ab}} \tag{B24}$$

$$\begin{aligned} \implies \sigma^{56} = \frac{2\pi e^3}{\hbar^2\omega^2}\int [d\mathbf{k}] f_{ba}\left[\frac{h^\alpha_{ba}h^\alpha_{ac}h^\mu_{cb}}{\varepsilon_{bc}} - \frac{h^\alpha_{ca}h^\alpha_{ab}h^\mu_{bc}}{\varepsilon_{cb}} + \frac{h^\alpha_{ab}h^\alpha_{bc}h^\mu_{ca}}{\varepsilon_{ac}} - \frac{h^\alpha_{cb}h^\alpha_{ba}h^\mu_{ac}}{\varepsilon_{ca}}\right] P\left(\frac{1}{\omega - \varepsilon_{ab}}\right) \\ + \frac{2\pi e^3}{\hbar^2\omega^2}\int [d\mathbf{k}] f_{ba}\left[\frac{h^\alpha_{ba}h^\alpha_{ac}h^\mu_{cb}}{\varepsilon_{bc}} + \frac{h^\alpha_{ca}h^\alpha_{ab}h^\mu_{bc}}{\varepsilon_{cb}} - \frac{h^\alpha_{ab}h^\alpha_{bc}h^\mu_{ca}}{\varepsilon_{ac}} - \frac{h^\alpha_{cb}h^\alpha_{ba}h^\mu_{ac}}{\varepsilon_{ca}}\right] i\pi\delta(\omega - \varepsilon_{ab}). \end{aligned} \tag{B25}$$

Now, the term involving $\delta(\omega - \varepsilon_{ab})$ can be written as

$$\sigma^{56}_{\delta(\omega-\varepsilon_{ab})} = \frac{2\pi e^3}{\hbar^2\omega^2}\int [d\mathbf{k}] f_{ba}\left[\frac{h^\alpha_{ba}h^\alpha_{ad}h^\mu_{db}}{\varepsilon_{bd}} + \frac{h^\alpha_{da}h^\alpha_{ab}h^\mu_{bd}}{\varepsilon_{db}} - \frac{h^\alpha_{ab}h^\alpha_{bd}h^\mu_{da}}{\varepsilon_{ad}} - \frac{h^\alpha_{db}h^\alpha_{ba}h^\mu_{ad}}{\varepsilon_{da}}\right] i\pi\delta(\omega - \varepsilon_{ab}) \tag{B26}$$

After rearranging these terms and using $\Delta^\alpha_{ab} = h^\alpha_{aa} - h^\alpha_{bb}$, we get

$$\begin{aligned} \sigma^{56}_{\delta(\omega-\varepsilon_{ab})} = \boxed{(-1)\frac{2\pi e^3}{\hbar^2\omega^2}\int [d\mathbf{k}] f_{ab}\Delta^\alpha_{ab}\left[\frac{h^\alpha_{ab}h^\mu_{ba}}{\varepsilon_{ab}} + \frac{h^\alpha_{ba}h^\mu_{ab}}{\varepsilon_{ba}}\right] i\pi\delta(\omega - \varepsilon_{ab})} \\ + \boxed{(-1)\frac{2\pi e^3}{\hbar^2\omega^2}\int [d\mathbf{k}] f_{ab}\sum_{d\neq a,b}\left[-\frac{h^\alpha_{da}h^\alpha_{ab}h^\mu_{bd}}{\varepsilon_{bd}} + \frac{h^\alpha_{db}h^\alpha_{ba}h^\mu_{ad}}{\varepsilon_{ad}} + \frac{h^\alpha_{ab}h^\alpha_{bd}h^\mu_{da}}{\varepsilon_{da}} - \frac{h^\alpha_{ba}h^\alpha_{ad}h^\mu_{db}}{\varepsilon_{db}}\right] i\pi\delta(\omega - \varepsilon_{ab})}. \end{aligned} \tag{B27}$$

Now, we can see that the above expression $\sigma^{56}_{\delta(\omega-\varepsilon_{ab})}$ is equal and opposite to the boxed part (three velocity terms) of Eq. B22. In other words:

$$\sigma^{23}_{\delta(\omega-\varepsilon_{ab})} + \sigma^{56}_{\delta(\omega-\varepsilon_{ab})} = \frac{2\pi e^3}{\hbar^2}\int [d\mathbf{k}] f_{ab}|\mathbf{A}^\alpha_{ab}|^2\mathbf{S}^{\mu\alpha}_{ba}\delta(\omega - \varepsilon_{ab}) \tag{B28}$$

which is the shift-current expression used in the main text.

Appendix C: Group Theoretical Analysis for second-order conductivity

In this section, we perform a group theoretical analysis to predict the non-zero components of second-order conductivity tensor for twisted bilayer graphene. If we consider a TBG encapsulated with hBN from both sides such that the sublattice symmetry breaking effect is same on both layers, we have $\Delta_1 = \Delta_2$. In this case, the symmetry group of TBG is D_3 generated by C_{3z} and C_{2y}. In our simulations, we found that there is only one independent component of $\sigma^\mu_{\alpha\beta}$ tensor when $\Delta_1 = \Delta_2$. It can be directly deduced from the number of cubic functions associated with the trivial irrep A_1 in the character table of D_3 shown in Tab. I [12].

Irreps	E	$2C_{3z}$	$3C_{2y}$	Linear functions	Quadratic functions	Cubic functions
A_1	1	1	1	-	$x^2 + y^2$, z^2	$y(y^2 - 3x^2)$
A_2	1	1	-1	z, R_z	-	$z^3, x(3y^2 - x^2), z(x^2 + y^2)$
E	2	-1	0	$(x, y), (R_x, R_y)$	$(y^2 - x^2, xy)(xz, yz)$	(xz^2, yz^2) $[xyz, z(y^2 - x^2)]$ $[y(x^2 + y^2), x(x^2 + y^2)]$

TABLE I. Character table for point group D_3 generated by C_{3z} and C_{2y}.

Irreps	e	c	c^2	Linear functions	Quadratic functions	Cubic functions
A_1	1	1	1	z	$x^2 + y^2$, z^2	z^3,$y(y^2 - 3x^2)$,$y(y^2 - 3x^2)$,$z(x^2 + y^2)$
E	1 1	$e^{i\frac{2\pi}{3}}$ $e^{-i\frac{2\pi}{3}}$	$e^{-i\frac{2\pi}{3}}$ $e^{i\frac{2\pi}{3}}$	$x + iy, R_x + iR_y$ $x - iy, R_x - iR_y$	$(x^2 - y^2, xy)$ (yz, xz)	(xz^2, yz^2) $[xyz, z(x^2 - y^2)]$ $[x(x^2 + y^2), y(x^2 + y^2)]$

TABLE II. Character table for point group C_{3z}.

It indicates that the second order tensor $\sigma^{\mu}_{\alpha\beta}$ has only one independent element with

$$\begin{aligned} \sigma^{y}_{xx} &= -\sigma^{y}_{yy} = \sigma^{y}_{xy} = \sigma^{x}_{yx} \neq 0 \\ \sigma^{x}_{yy} &= -\sigma^{x}_{xx} = \sigma^{y}_{yx} = \sigma^{y}_{xy} = 0. \end{aligned} \tag{C1}$$

On the other hand, as shown in table II, the trivial irrep for C_{3z} has two cubic functions (ignoring the ones involving z as our system is two dimensional only) indicating that a rank three tensor can have two independent components under C_3. As a result of this, for $\Delta_1 \neq \Delta_2$, we have

$$\begin{aligned} \sigma^{y}_{xx} &= -\sigma^{y}_{yy} = \sigma^{y}_{xy} = \sigma^{x}_{yx} \neq 0 \\ \sigma^{x}_{yy} &= -\sigma^{x}_{xx} = \sigma^{y}_{yx} = \sigma^{y}_{xy} \neq 0 \end{aligned} \tag{C2}$$

which is consistent with our observation in Fig. S3.

Helicity dependent current in TBG

The second-order CPGE is captured by a rank two tensor (not a rank three tensor like shift-current response)

$$j_\alpha = i\eta_{\alpha\beta}(\mathbf{E} \times \mathbf{E}^*)_\beta. \tag{C3}$$

If we consider a two-dimensional material in $x-y$ plane, then the normal incidence results in $\beta = z$ and the in-plane current requires $\alpha = x, y$. Now, the quantity $(\mathbf{E} \times \mathbf{E}^*)_z$ is the z component of an axial vector which shares representation A_1 in C_{3z} character table II (denoted by R_z in the character table). On the other hand, the electric current $\mathbf{j} = j_x\widehat{\mathbf{x}} + j_y\widehat{\mathbf{y}}$ is a polar vector which has irrep E, and thus the CPGE conductivity tensor, $n_{\alpha\beta}$ transforms according to irrep $A_1 \otimes E = E$ which contains no trivial irrep A_1, and thus $n_{\alpha z} = 0$. However, if we consider an oblique incidence (i.e $\beta = x, y$), then we might get a non-zero component but this needs an electric field with z component. Now, in the minimal coupling picture, we do not have a momentum component in this direction and E_z cannot couple to our system and thus CPGE can not occur. However, it can couple to the layer degree of freedom which would be an interesting direction to pursue but we need to go beyond the minimal coupling approach which is beyond the scope of this current work. However, if the symmetry is lowered to a reflection symmetry with a mirror plane perpendicular to the plane of the bilayer graphene, it can result in a non-zero injection current from circularly polarized light.

Appendix D: Charge density profile

We propose that the large shift-current response observed for the twisted bilayer graphene in this work is related to changes in the spatial distribution associated with the Bloch wavefunction when excited from one band to another. The Bloch states originating from different regions of the mini-BZ and bands give rise to a different charge density profile. We compute the local charge density profile,

$$n(\mathbf{r}, E) = \sum_{n,\mathbf{k}} \Psi^{\dagger}_{n\mathbf{k}}(\mathbf{r})\Psi_{n\mathbf{k}}(\mathbf{r})\delta(E - \varepsilon_{n,\mathbf{k}})\,, \tag{D1}$$

where $n, \mathbf{k}$ label the band and momentum point respectively. Here $\Psi_{n\mathbf{k}}(\mathbf{r})$ corresponds to the Bloch eigenstate of the mean-field Hamiltonian of Sec. III with an eigenvalue $\varepsilon_{n,\mathbf{k}}$ and $\mathbf{r}$ tracks the position in real space ($\mathbf{r} = 0$ corresponds to the AA site).

Animation showing distribution of charge originating from states in a narrow energy window for $\theta = 0.8°$ is shown in the Supplemental Material Video "charge_density_profile.mp4". We highlight the varying structure of charge densities centered near AA sites and in rings surrounding AA sites and the corresponding energies. Whenever a transition from a state centered near AA site to a ring-like state occurs, corresponding energy difference between these states matches sharp resonances in Fig.1f of the main text. A precise relation between this observation and the enhanced resonance peaks remains to be explored in a future work.

[1] Y. Choi, H. Kim, C. Lewandowski, Y. Peng, A. Thomson, R. Polski, Y. Zhang, K. Watanabe, T. Taniguchi, J. Alicea, *et al.*, Nature Physics **17**, 1375–1381 (2021).

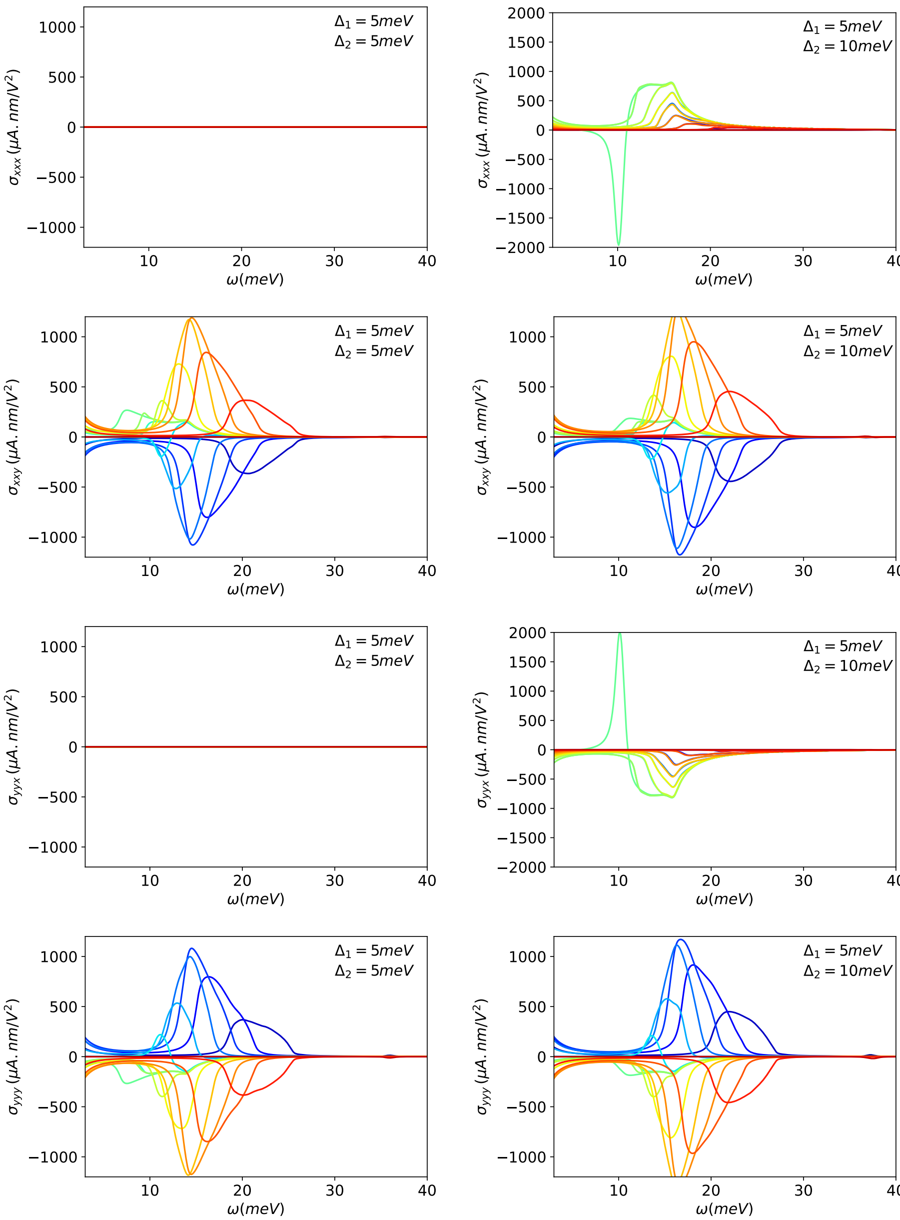

Supplemental Figure S3. **Effect of C_{2y} symmetry breaking on different shift-current responses.** Second-order conductivity tensor elements, σ_{xxx},σ_{xxy}, σ_{yyx}, and σ_{yyy} for $\Delta_1 = \Delta_2 = \Delta$ case (left column) and for $\Delta_1 \neq \Delta_2$ (right column). We notice that breaking C_{2y} by choosing different values for Δ_1 and Δ_2 results in a non-zero value for σ_{xxx} and σ_{yyy}.

[2] T. Cea, N. R. Walet, and F. Guinea, Physical Review B **100**, 205113 (2019).
[3] T. Cea and F. Guinea, Physical Review B **102**, 045107 (2020).
[4] N. Bultinck, E. Khalaf, S. Liu, S. Chatterjee, A. Vishwanath, and M. P. Zaletel, Physical Review X **10**, 031034 (2020).
[5] E. Khalaf, S. Chatterjee, N. Bultinck, M. P. Zaletel, and A. Vishwanath, Science advances **7**, eabf5299 (2021).
[6] M. Xie and A. H. MacDonald, Phys. Rev. Lett. **124**, 097601 (2020).
[7] M. Xie and A. H. MacDonald, arXiv:2010.07928 [cond-mat] (2020), arXiv:2010.07928 [cond-mat].
[8] S. Carr, S. Fang, Z. Zhu, and E. Kaxiras, Phys. Rev. Research **1**, 013001 (2019).
[9] W. Qin, B. Zou, and A. H. MacDonald, arXiv preprint arXiv:2102.10504 (2021).
[10] F. Guinea and N. R. Walet, Proceedings of the National Academy of Sciences **115**, 13174 (2018).
[11] D. E. Parker, T. Morimoto, J. Orenstein, and J. E. Moore, Phys. Rev. B **99**, 045121 (2019).
[12] M. S. Dresselhaus, G. Dresselhaus, and A. Jorio, *Group theory: application to the physics of condensed matter* (Springer Science & Business Media, 2007).